

# Lethal synergy between SARS-CoV-2 and *Streptococcus pneumoniae* in hACE2 mice and protective efficacy of vaccination

Tarani Kanta Barman, Amit K. Singh, Jesse L. Bonin, Tanvir Noor Nafiz, Sharon L. Salmon, and Dennis W. Metzger

Department of Immunology and Microbial Disease, Albany Medical College, Albany, New York, USA.

Secondary infections are frequent complications of viral respiratory infections, but the potential consequence of SARS-CoV-2 coinfection with common pulmonary pathogens is poorly understood. We report that coinfection of human ACE2-transgenic mice with sublethal doses of SARS-CoV-2 and *Streptococcus pneumoniae* results in synergistic lung inflammation and lethality. Mortality was observed regardless of whether SARS-CoV-2 challenge occurred before or after establishment of sublethal pneumococcal infection. Increased bacterial levels following coinfection were associated with alveolar macrophage depletion, and treatment with murine GM-CSF reduced numbers of lung bacteria and pathology and partially protected from death. However, therapeutic targeting of IFNs, an approach that is effective against influenza coinfections, failed to increase survival. Combined vaccination against both SARS-CoV-2 and pneumococci resulted in 100% protection against subsequent coinfection. The results indicate that when seasonal respiratory infections return to pre-pandemic levels, they could lead to an increased incidence of lethal COVID-19 superinfections, especially among the unvaccinated population.

## Introduction

Coinfections with both pulmonary viral and bacterial pathogens often lead to synergistic lethality, but little is understood about the interplay between severe acute respiratory syndrome coronavirus 2 (SARS-CoV-2) and common pathogens such as *Streptococcus pneumoniae* (1). The frequency of SARS-CoV-2 and bacterial coinfection among hospitalized patients has been estimated to be approximately 7% (2). With the lifting of pandemic restrictions, including social isolation, masking, and frequent surface decontamination, cases of respiratory infection may return to historic pre-pandemic levels and lead to a heightened incidence of coinfections. When described, bacterial coinfections during COVID-19 have been described to be associated with increased risk of shock, respiratory failure, and a prolonged stay in intensive care (3). In addition, it appears that there can be increased mortality of patients with COVID-19 owing to secondary bacterial infections, despite antibiotic therapy (4, 5); this is possibly associated with cases of antibiotic resistance (6). It is therefore critical to understand the potential effect of SARS-CoV-2 coinfection with other pulmonary pathogens such as *S. pneumoniae* (1).

Likewise, it is important to establish measures that might ameliorate the impact of SARS-Cov-2 coinfections. Administration of GM-CSF as well as neutralization of IFNs have shown promise in murine models of influenza virus/*S. pneumoniae* pulmonary coinfections (7, 8). In addition, mRNA vaccines have demonstrated 90%–95% protection against human COVID-19 (9, 10). However, the efficacy of these approaches in the setting of coinfection with SARS-CoV-2 and *S. pneumoniae* is not known. Here, we report that coinfection of human angiotensin-converting enzyme II-transgenic (ACE2-transgenic) mice with sublethal doses of SARS-CoV-2 and *S. pneumoniae* results in synergistic superinfection and lethality. Treatment with GM-CSF provided moderate protection against synergistic disease, while vaccination against both SARS-CoV-2 and *S. pneumoniae* induced 100% protection.

## Results

*Proinflammatory cytokine and innate cell levels in lungs of SARS-CoV-2/S. pneumoniae-coinfected hACE2 mice.* This study was specifically designed to investigate the consequences of SARS-CoV-2/*S. pneumoniae* coinfection on morbidity and mortality, using the human ACE2 receptor-transgenic (hACE2-transgenic)

**Conflict of interest:** The authors have declared that no conflict of interest exists.

**Copyright:** © 2022, Barman et al. This is an open access article published under the terms of the Creative Commons Attribution 4.0 International License.

**Submitted:** February 16, 2022

**Accepted:** April 26, 2022

**Published:** June 8, 2022

**Reference information:** JCI Insight. 2022;7(11):e159422.  
<https://doi.org/10.1172/jci.insight.159422>.

mouse model (11). Briefly, mice were intranasally (i.n.) infected with a sublethal dose of SARS-CoV-2 on day 0, followed by sublethal i.n. challenge with *S. pneumoniae* on day 6 (Figure 1A). This coinfection procedure is similar to that typically used in mice to model human influenza virus/bacteria coinfections (12, 13) Three days after *S. pneumoniae* challenge, proinflammatory cytokine expression in the bronchoalveolar lavage fluid (BALF) was measured. Mice infected with sublethal doses of either SARS-CoV-2 or *S. pneumoniae* alone had BALF cytokine levels that were essentially equivalent to those of naive mice (Figure 1B). However, coinfecting mice expressed significantly greater cytokine levels, including very high amounts of IL-6, MIP-1 $\alpha$ , and TNF- $\alpha$ . Innate immune cell infiltration into the bronchoalveolar lavage (BAL) and lung tissues was also measured using typical gating strategies for murine pulmonary immune cells (Supplemental Figure 1, A and B; supplemental material available online with this article; <https://doi.org/10.1172/jci.insight.159422DS1>). Singly infected mice showed levels of BAL and lung cells that were similar to those of naive mice. However, 3 days following coinfection with *S. pneumoniae*, striking increases in inflammatory cells, including monocytes, neutrophils, NK cells, and dendritic cells, were observed (Figure 1, C–J; Supplemental Figure 1, C and D; and Supplemental Figure 2, A–D). There was also a slight increase in dendritic cell numbers in mice infected with SARS-CoV-2 alone (Figure 1, I and J). Simultaneously, alveolar macrophages were depleted after SARS-CoV-2 infection (Figure 1, K and L, and Supplemental Figure 2, E and F). We also quantified CD4<sup>+</sup> and CD8<sup>+</sup> T cell levels but did not observe any significant differences among the groups (data not shown).

*Viral/bacterial loads, histopathology, and lethality in SARS-CoV-2/S. pneumoniae-coinfecting hACE2 mice.* Our results showed that even mild SARS-CoV-2 infection combined with sublethal *S. pneumoniae* coinfection can cause a cytokine storm and major shifts in levels of innate cell levels in the lungs. We next examined pathogen loads, tissue pathology, and survival of SARS-CoV-2/*S. pneumoniae*-coinfecting mice (Figure 2A). In hACE2 mice infected with *S. pneumoniae* alone, the bacteria appeared to persist but not replicate, while, in coinfecting mice, the bacterial numbers increased and were approximately 10<sup>5</sup> greater within 72 hours, compared with the original challenge dose (Figure 2B). This defect in controlling infection was consistent with the observed depletion of resident alveolar macrophages after SARS-CoV-2 challenge (Figure 1, K and L) (14, 15). Levels of replicating SARS-CoV-2 were also significantly elevated within 3 days after *S. pneumoniae* coinfection, as assessed by PFU formation in Vero cell cultures (Figure 2C). These increases in pathogen levels were associated with severe interstitial pneumonia, hemorrhage, epithelial desquamation, diffuse alveolar damage, and loss of normal lung tissue architecture (Figure 2D), similar to that reported for severe COVID-19 disease in mice (11). Histopathology of naive mice and mice sublethally infected with either pathogen alone appeared to be essentially normal (Figure 2D), and scoring of the tissue sections showed that pathology was significantly greater in SARS-CoV-2/*S. pneumoniae*-coinfecting mice compared with mice infected with either pathogen alone (Figure 2E). The pathological changes seen in coinfecting animals were fully consistent with the increased expression of lung proinflammatory cytokines and innate cell populations (Figure 1).

We next evaluated survival outcomes using two different models of SARS-CoV-2/*S. pneumoniae* coinfection. It is known that the sequence of influenza virus/bacteria coinfection plays an important role in humans (16). Thus, we first used a model in which mice were infected with a relatively low dose of SARS-CoV-2 virus, followed 6 days later with a sublethal *S. pneumoniae* challenge, as in the above experiments. While mice infected with only SARS-CoV-2 or *S. pneumoniae* had minimal weight loss and 100% survival, coinfecting mice lost more than 20% of their weight and all succumbed within 5 days after *S. pneumoniae* challenge (Figure 2, F and G). Because *S. pneumoniae* is typically a human commensal restricted to the upper respiratory tract, in further experiments we colonized mice with *S. pneumoniae* on day 0, followed by SARS-CoV-2 challenge on day 2, similar to our previous work with murine *S. pneumoniae*/influenza virus coinfection (7). *S. pneumoniae*/SARS-CoV-2 coinfection using this challenge schedule led to minimal weight loss but still induced 60% mortality; again, singly infected mice all survived (Figure 2, H and I).

*Treatment with GM-CSF for SARS-CoV-2/S. pneumoniae coinfection.* The beneficial effects of GM-CSF in animal models of bacterial and viral lung infections, including influenza virus/*S. pneumoniae* coinfections, have been reported by several investigators (8, 17–23). For SARS-CoV-2 infection, clinical trials of GM-CSF therapy are ongoing (23). Because our results showed that SARS-CoV-2/*S. pneumoniae* coinfection led to depletion of alveolar macrophages and subsequent outgrowth of pneumococcus, we hypothesized that GM-CSF treatment might stabilize alveolar macrophage expression and protect against SARS-CoV-2/*S. pneumoniae* infection by enhancing pathogen clearance and/or tissue repair mechanisms. Treatment with

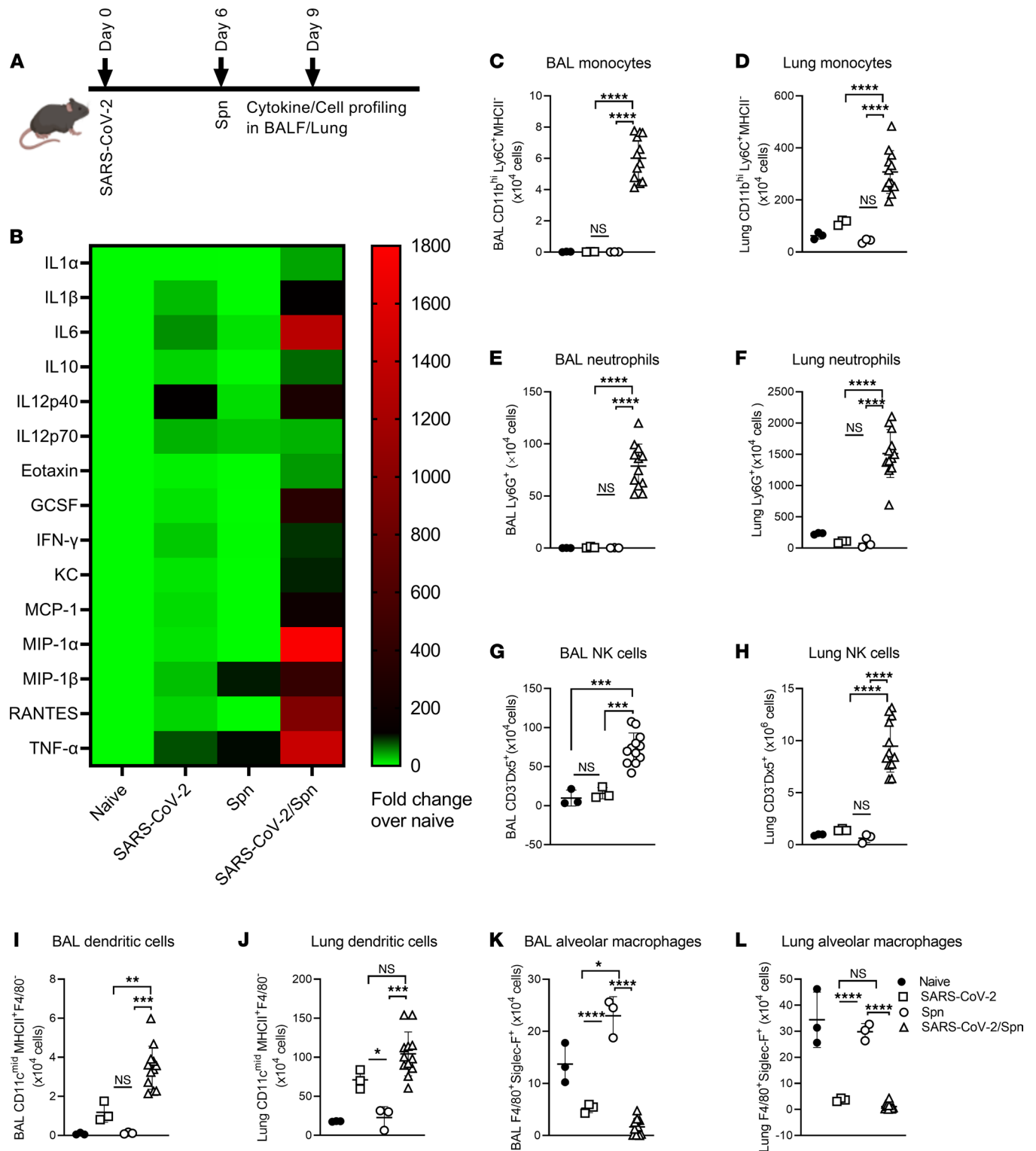


**Figure 1. Proinflammatory cytokine and innate immune cell levels in SARS-CoV-2/*S. pneumoniae*-coinfected hACE2 mice.** (A) Experimental design. (B) Cytokine levels in the BALF of SARS-CoV-2/*S. pneumoniae*-coinfected hACE2 mice. (C–L) Innate immune cell profiles in BAL and lung tissues from SARS-CoV-2/*S. pneumoniae*-coinfected hACE2 mice: (C and D) monocytes, (E and F) neutrophils, (G and H) NK cells, (I and J) dendritic cells, and (K and L) alveolar macrophages. Data are pooled from 2 independent experiments and presented as mean  $\pm$  SD.  $n = 3–6$  mice per group per experiment; each symbol represents a single mouse. Data were analyzed by ANOVA with Tukey’s multiple comparisons post hoc test. \* $P < 0.05$ , \*\* $P < 0.01$ , \*\*\* $P < 0.001$ , \*\*\*\* $P < 0.0001$ . Spn, *S. pneumoniae*

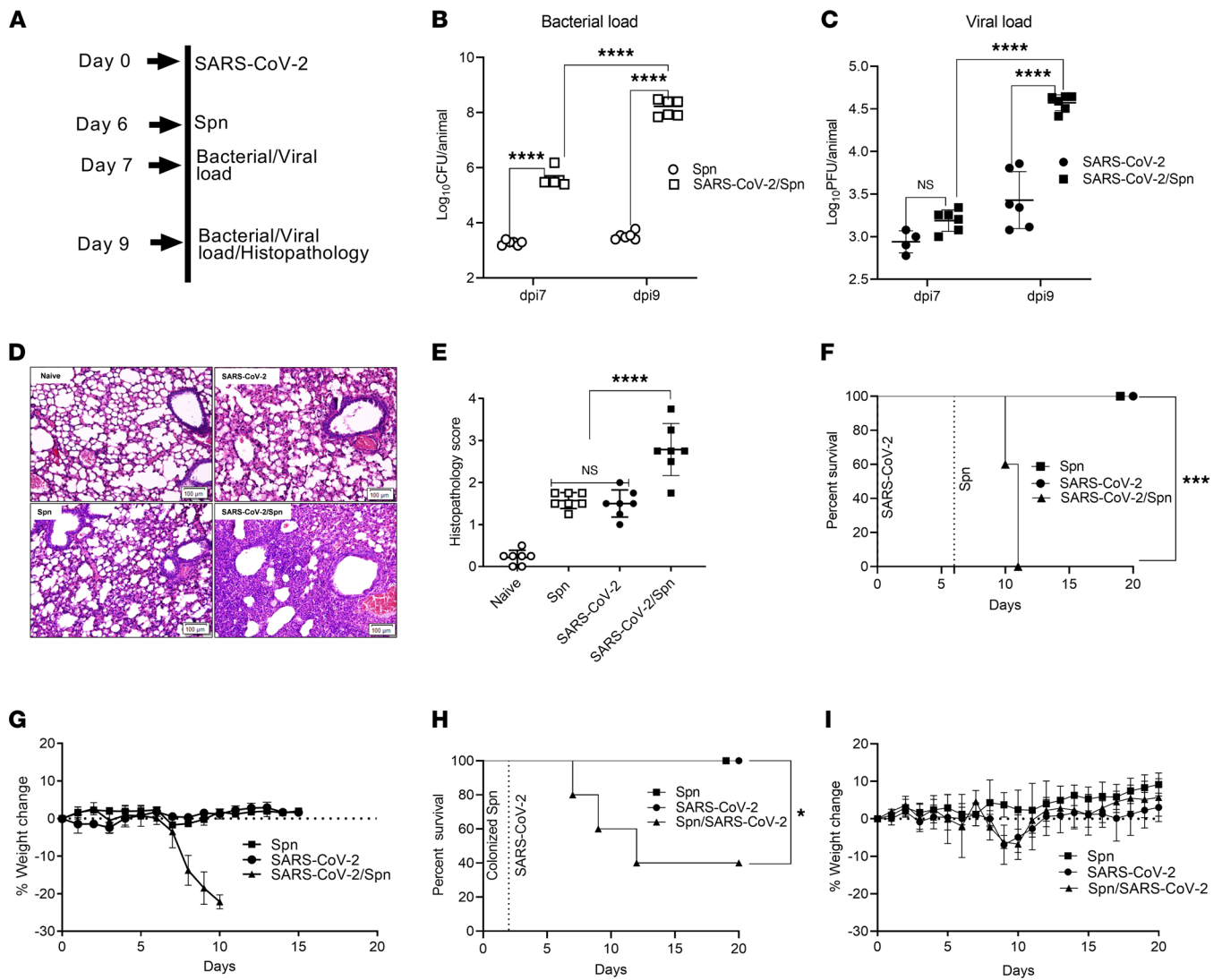


**Figure 2. Viral/bacterial loads, histopathology, morbidity, and mortality in SARS-CoV-2/*S. pneumoniae*-coinfected hACE mice.** (A) Experimental design. (B) Bacterial CFUs in lung homogenates.  $n = 6$  mice per group. (C) Viral PFUs in lung homogenates.  $n = 6$  mice per group. (B and C) Data were analyzed by ANOVA with Tukey's multiple comparisons post hoc test. (D) Representative H&E staining of lung tissues in naive, *S. pneumoniae*-, SARS-CoV-2-, and SARS-CoV-2/*S. pneumoniae*-coinfected hACE2 mice.  $n = 3$  mice per group. Original magnification,  $\times 20$ . Scale bar: 100  $\mu$ m. (E) Histopathology scores. The data were analyzed by ANOVA with Tukey's multiple comparisons post hoc test. (F–I) Morbidity and mortality following SARS-CoV-2 and *S. pneumoniae* coinfection. SARS-CoV-2/*S. pneumoniae* coinfection (F) survival and (G) weight loss. *S. pneumoniae*/SARS-CoV-2 coinfection (H) survival and (I) weight loss. In each experiment  $n = 5$  mice per group. Survival data were analyzed by the log-rank Mantel-Cox test. \* $P < 0.05$ , \*\*\* $P < 0.001$ , \*\*\*\* $P < 0.0001$ . Spn, *S. pneumoniae*.

GM-CSF during SARS-CoV-2 infection but before challenge with *S. pneumoniae* led to decreased BALF cytokine levels compared with PBS-treated coinfecting mice (Figure 3A). Levels of inflammatory cell populations, including monocytes, neutrophils, NK cells, and dendritic cells, were also decreased in GM-CSF-treated coinfecting mice as compared with the control PBS-treated group (Figure 3, B–D). However, levels of alveolar macrophages in both in BAL and lung tissue were increased following GM-CSF treatment (Figure 3, J and K). Consistent with enhanced expression of alveolar macrophages, bacterial cell counts were significantly decreased in lung tissues of GM-CSF-treated mice (Figure 3L). In addition, in some but not all mice, viral PFU levels were reduced (Figure 3M). Histopathology analysis indicated that inflammatory infiltrates and interstitial pneumonia were mild to moderate in GM-CSF-treated mice compared with the severe pathology seen in PBS-treated coinfecting mice (Figure 3N). Finally, although all mice initially lost weight, mortality was slightly delayed in GM-CSF-treated mice, and 25% of the mice survived coinfection, while all coinfecting mice treated with PBS died by day 11 (Figure 3, O and P).

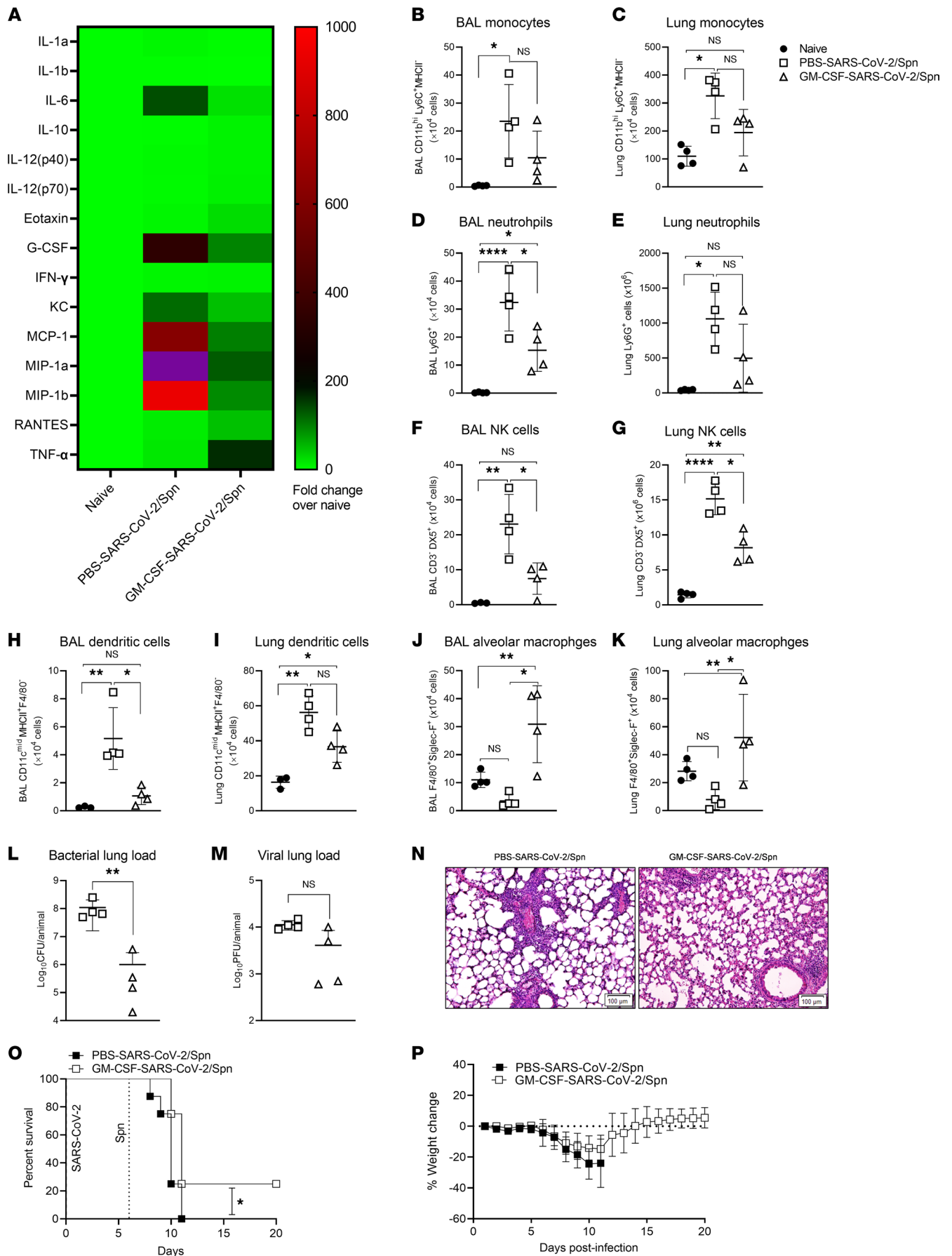


**Figure 3. Treatment with GM-CSF for SARS-CoV-2/*S. pneumoniae* coinfection.** (A) Cytokine levels in the BALF of SARS-CoV-2/*S. pneumoniae*-coinfected hACE2 mice treated with PBS or GM-CSF. (B–K) Innate immune cell profiles in BAL and lung tissues from SARS-CoV-2/*S. pneumoniae*-coinfected hACE2 mice treated with PBS or GM-CSF: (B and C) monocytes, (D and E) neutrophils, (F and G) NK cells, (H and I) dendritic cells, and (J and K) alveolar macrophages. (L) Bacterial CFU and (M) viral PFU in lung homogenates following PBS or GM-CSF treatment.  $n = 4$  mice per group. (N) Representative H&E staining of lung tissues from SARS-CoV-2/*S. pneumoniae*-coinfected hACE2 mice with PBS and GM-CSF treatment.  $n = 3$  mice per group. Original magnification,  $\times 20$ . Scale bar: 100  $\mu\text{m}$ . (O) Survival and (P) weight loss in SARS-CoV-2/*S. pneumoniae*-coinfected mice following PBS or GM-CSF treatment.  $n = 7$ –8 mice per group. Survival data were analyzed by the log-rank Mantel-Cox test. All other data were analyzed by ANOVA with Tukey's multiple comparisons post hoc test. \* $P < 0.05$ , \*\* $P < 0.01$ , \*\*\*\* $P < 0.0001$ . Spn, *S. pneumoniae*.

*Therapeutic neutralization of IFN- $\alpha$ βR, IFN- $\gamma$ , and TNF- $\alpha$ , in SARS-CoV-2/*S. pneumoniae* coinfecting hACE2 mice.* It is known that neutralization of type I and II IFN signaling can significantly increase survival following influenza virus/*S. pneumoniae* coinfection (7). Previous studies in hACE2-transgenic mice have also reported that neutralization of IFN- $\gamma$  when combined with anti-TNF- $\alpha$  mAb treatment can rescue mice from pathology after infection with SARS-CoV-2 alone (24). We therefore tested the protective efficacy of various combinations of these neutralizing mAbs in models of both SARS-CoV-2/*S. pneumoniae* and *S. pneumoniae*/SARS-CoV-2 coinfection, using the same conditions for cytokine neutralization as in previous studies (24). However, we observed no effects on morbidity or mortality (Figure 4). A single mouse in the anti-IFN- $\gamma$ /TNF- $\alpha$ -treated group survived, but this was likely stochastic, as all other mice in this group died within the same time frame as the IgG isotype control group (as well as in all of the other mAb-treated groups, including mice triply treated with anti-IFN- $\alpha$ βR/IFN- $\gamma$ /TNF- $\alpha$ ). We conclude that neutralization of these proinflammatory cytokines is unlikely to prevent lethal synergy that might be seen during SARS-CoV-2 coinfections.

*Efficacy of vaccination for protection against SARS-CoV-2/*S. pneumoniae* coinfection.* To assess the protective value of vaccination, individual groups of mice were immunized against either *S. pneumoniae* or SARS-CoV-2 and then infected after 28 days with SARS-CoV-2, followed 6 days later with *S. pneumoniae* (Figure 5A). In all cases, serum antibodies reached levels 21 days after vaccination that were sufficient for protection against the relevant single pathogen (minimum 50% serum antibody titer of  $>200$ ) (25, 26) (Figure 5, B and C). For SARS-CoV-2/*S. pneumoniae* coinfection, we found that vaccination with the Pfizer mRNA COVID-19 vaccine provided approximately 50% protection (Figure 5, D and E). A similar level of protection was seen after vaccination with the Prevnar13 *S. pneumoniae* vaccine (Figure 5, D and E). However, dual vaccination with both Pfizer mRNA COVID-19 vaccine and Prevnar13 *S. pneumoniae* vaccine resulted in 100% survival against SARS-CoV-2/*S. pneumoniae* coinfection (Figure 5, D and E).

*Correlates of vaccine efficacy for protection against SARS-CoV-2/*S. pneumoniae* coinfection.* We next examined potential correlates of protection in vaccinated mice. During SARS-CoV-2/*S. pneumoniae* coinfection of naive mice, the most striking features associated with lethality were cytokine storm and increased infiltration of monocytes, neutrophils, NK cells, and dendritic cells, in conjunction with a marked decrease in numbers of alveolar macrophages (Figure 1). After challenge of vaccinated hACE2 mice with SARS-CoV-2/*S. pneumoniae*, several proinflammatory cytokines that were highly expressed in unvaccinated coinfecting mice were significantly reduced, and infiltration of monocytes, neutrophils, NK cells, and dendritic cells was likewise reduced (Figure 6, A–I). Concurrently, levels of alveolar macrophages were increased in challenged, vaccinated mice (Figure 6, J and K). The maximum increase in alveolar macrophages was seen in mRNA COVID-19-vaccinated mice. Both viral and bacterial pulmonary loads were significantly decreased in vaccinated mice compared with unvaccinated coinfecting controls (Figure 6, L and M). The presence of histopathological lesions (Figure 6N) was consistent with our immune function findings — unvaccinated SARS-CoV-2/*S. pneumoniae*-coinfecting mice exhibited severe tissue pathology on day 9 compared with mice previously vaccinated with the Pfizer mRNA vaccine or Prevnar13. In the vaccinated mice, the lesions were mild (Figure 6N).

## Discussion

Our results demonstrated that coinfection of hACE2 mice with sublethal doses of SARS-CoV-2 and *S. pneumoniae* resulted in severe inflammation and lethality, while challenge with the same doses of SARS-CoV-2 or *S. pneumoniae* alone did not induce disease. Severe disease induced with SARS-CoV-2 can result in dysregulated inflammation and cytokine storm (27–31), and our results now show for the first time to our knowledge that cytokine storm can also be induced by mild SARS-CoV-2 infection when combined with *S. pneumoniae* superinfection. Coinfection was associated with infiltration of inflammatory cells into the lung and depletion

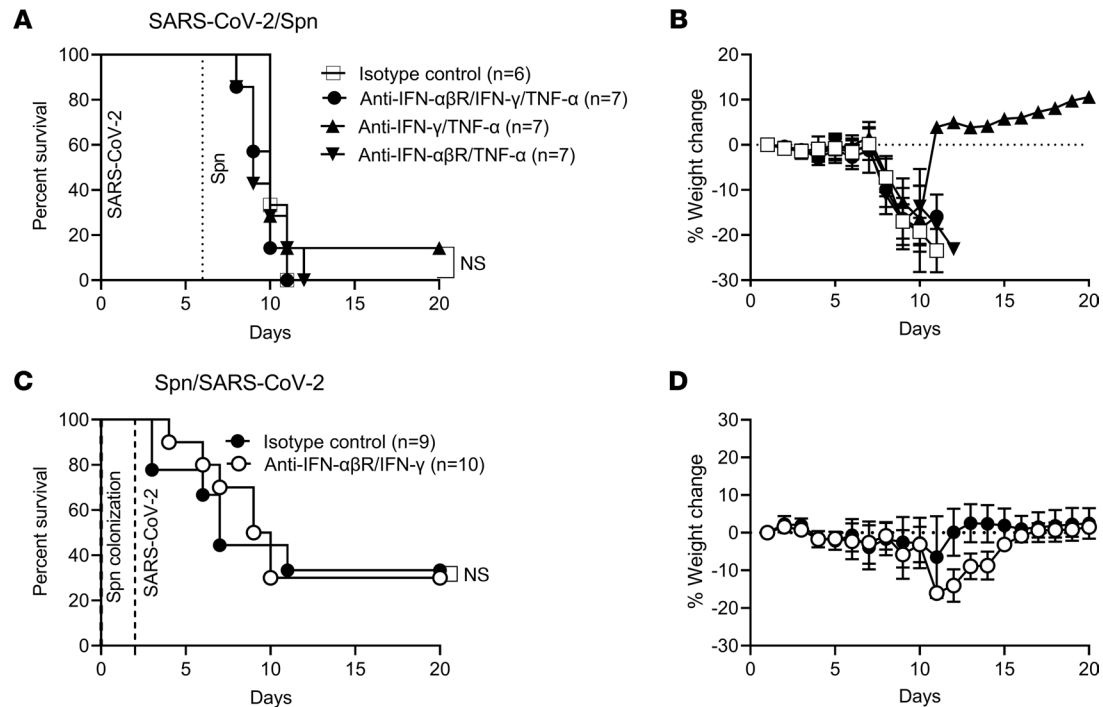


**Figure 4. Therapeutic neutralization of IFN- $\alpha\beta$ R, IFN- $\gamma$ , and TNF- $\alpha$  in SARS-CoV-2/*S. pneumoniae*-coinfected hACE2 mice. (A and B)** Survival and weight change after combined anti-IFN- $\alpha\beta$ R, anti-IFN- $\gamma$ , and anti-TNF- $\alpha$  mAb treatment during SARS-CoV-2/*S. pneumoniae* coinfection.  $n = 6$ – $7$  mice per group. **(C and D)** Combined anti-IFN- $\alpha\beta$ R and anti-IFN- $\gamma$  mAb treatment during *S. pneumoniae*/SARS-CoV-2 coinfection.  $n = 9$ – $10$  mice per group. Survival data were analyzed by the log-rank Mantel-Cox test. Spn, *S. pneumoniae*.

of resident alveolar macrophages. While neutralization of IFN and TNF- $\alpha$  signaling failed to provide protection, GM-CSF treatment did decrease pathology and allowed some mice to survive coinfection. In addition, dual vaccination against both SARS-CoV-2 and *S. pneumoniae* led to a protective efficacy of 100%.

In our study, levels of monocytes, neutrophils, NK cells, and dendritic cells were particularly increased in coinfecting mice compared with singly infected mice. However, alveolar macrophage levels were decreased. During SARS-CoV-2 infection, the majority of macrophages present in the lung are believed to arise from infiltrating monocytes (32, 33). However, in spite of a dramatic increase in monocytes, the levels of alveolar macrophages in our study did not increase proportionately. The cause and mechanisms of alveolar macrophage depletion need further investigation but based on studies in other coinfection models, it is likely to be due to activation-induced cell death. In coinfecting mice, we also observed in BALF and lung tissue large numbers of neutrophils, cells that are thought to play roles in pathology during COVID-19 (34) through production of several inflammatory cytokines (35) leading to tissue damage (36). We likewise observed increased numbers of NK cells during SARS-CoV-2/*S. pneumoniae* coinfection. While NK cells are believed to control SARS-CoV-2 infection and decreased numbers of NK cells correlate with disease severity and mortality of patients with COVID-19 (37), their role during coinfection is not known. Finally, our results showed that the number of dendritic cells was also increased in BALF and lung tissues of coinfecting mice. Dendritic cells are targets of SARS-CoV-2 infection and involved in innate and adaptive immunity (38), but their functional capabilities in superinfections have yet to be fully explored.

Both bacterial and viral loads were significantly increased during SARS-CoV-2/*S. pneumoniae* coinfection. We hypothesize that the overgrowth of *S. pneumoniae* was fueled by the decreased numbers of phagocytic alveolar macrophages, which, in turn, led to inflammatory cell infiltration, proinflammatory cytokine expression, and, ultimately, lethal tissue damage. Reduction in alveolar macrophage numbers following pulmonary influenza virus infection of mice has been previously reported (39, 40) in addition to changes in alveolar macrophage phenotype (12, 41). The resulting lung tissue lesions in coinfecting mice were characterized by severe interstitial pneumonia with inflammatory cell infiltration, hemorrhages, epithelial desquamation, diffuse alveolar damage, and loss of lung tissue architecture, as also seen in lethal COVID-19 of mice (11, 42) and humans (1).

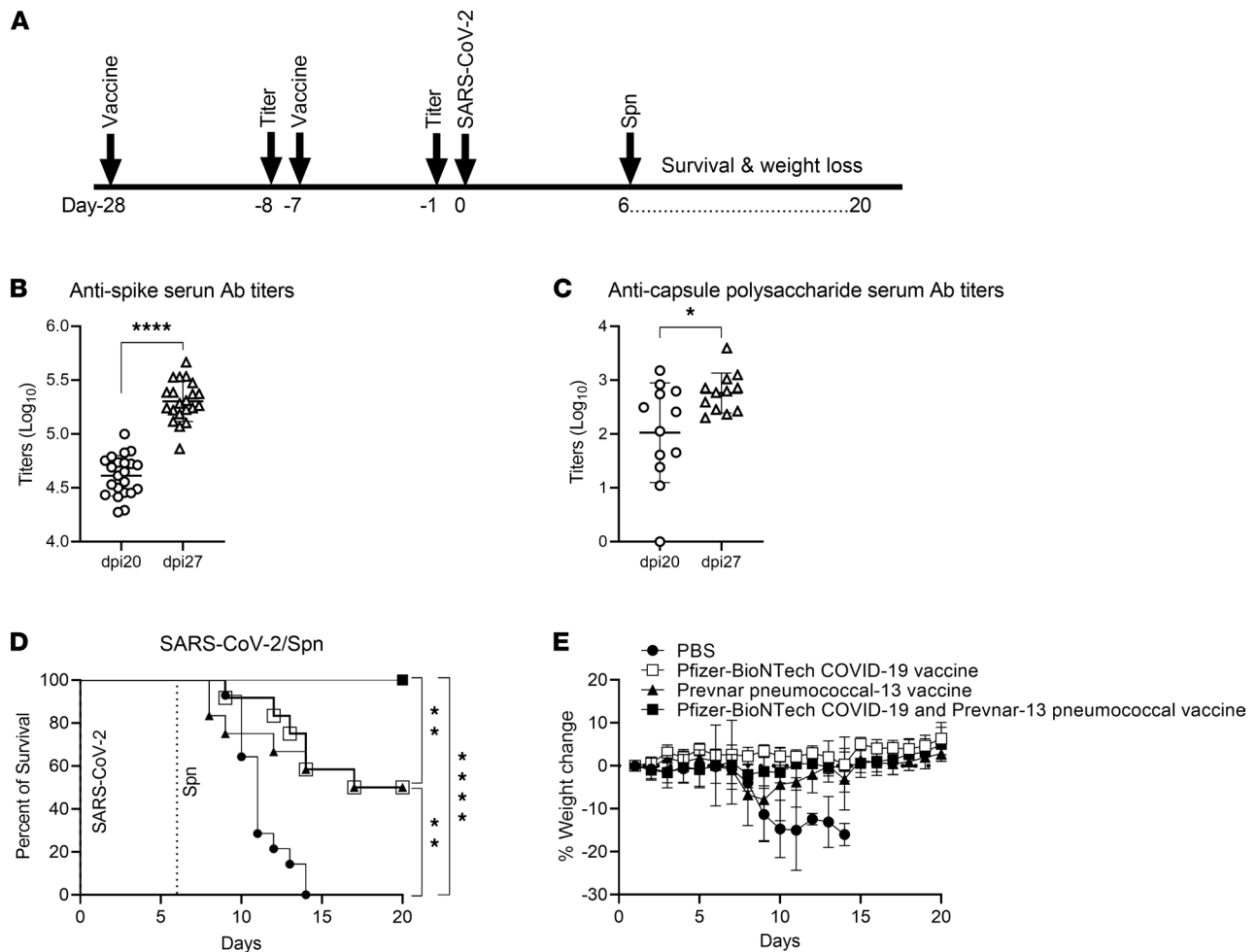


**Figure 5. Efficacy of vaccination for protection against SARS-CoV-2/*S. pneumoniae* coinfection.** (A) Experimental design. (B) Anti-spike serum antibody titers induced by the Pfizer-BioNTech COVID-19 vaccine, and (C) anti-pneumococcal polysaccharide serotype 3 serum antibody titers induced by the Pfizer Pevnar13 vaccine. Serum antibody titers from individual mice were determined by ELISA using 50% maximal binding as the titer endpoint.  $n = 11$ – $22$  mice per group pooled from 2 independent experiments. Protection in terms of (D) survival and (E) weight loss of hACE2 mice following SARS-CoV-2/*S. pneumoniae* coinfection by Pevnar13 pneumococcal conjugate vaccine, Pfizer mRNA vaccine, or dual Pevnar13 and Pfizer mRNA vaccines.  $n = 5$ – $8$  mice per group per experiment; data pooled from 2 independent experiments. Statistical analyses for survival were performed by the log-rank Mantel-Cox test. \* $P < 0.05$ , \*\*\*\* $P < 0.0001$ . Spn, *S. pneumoniae*. DPI, days post immunization.

All mice in our study that were initially infected with SARS-CoV-2 and then challenged 6 days later with *S. pneumoniae* succumbed by day 11. We determined whether reversing the sequence of coinfection — precolonization of mice with *S. pneumoniae* followed by SARS-CoV-2 infection, a situation most relevant to human infection, especially in children — would similarly lead to high levels of lethality. In this case, we reproducibly observed 60% mortality. It is worth noting that, in human influenza virus/*S. pneumoniae* coinfection, the sequence of pathogen exposure appears to play a critical role in disease progression (16).

SARS-CoV-2/*S. pneumoniae* coinfection induced synergistic lethality that was associated with depletion of macrophages and subsequent overgrowth of pneumococci. Therapeutic administration of GM-CSF before bacterial coinfection enhanced alveolar macrophage levels and resulted in decreased numbers of pneumococci in the lungs. This, in turn, led to decreased inflammatory cytokine expression in the lung and a moderate survival advantage. GM-CSF, an important pleiotropic cytokine and growth factor, plays a vital role in alveolar macrophage homeostasis, lung inflammation, and immunological disease. GM-CSF is known to serve a key role in normal physiology of lung health and can be important for host defense. GM-CSF acts locally on inflamed lung tissues to enhance growth, survival, and proliferation of alveolar macrophages. The beneficial effects of GM-CSF in animal models of bacterial and viral lung infection have been reported by many investigators (8, 17–22). For SARS-CoV-2 infection, clinical trials of GM-CSF

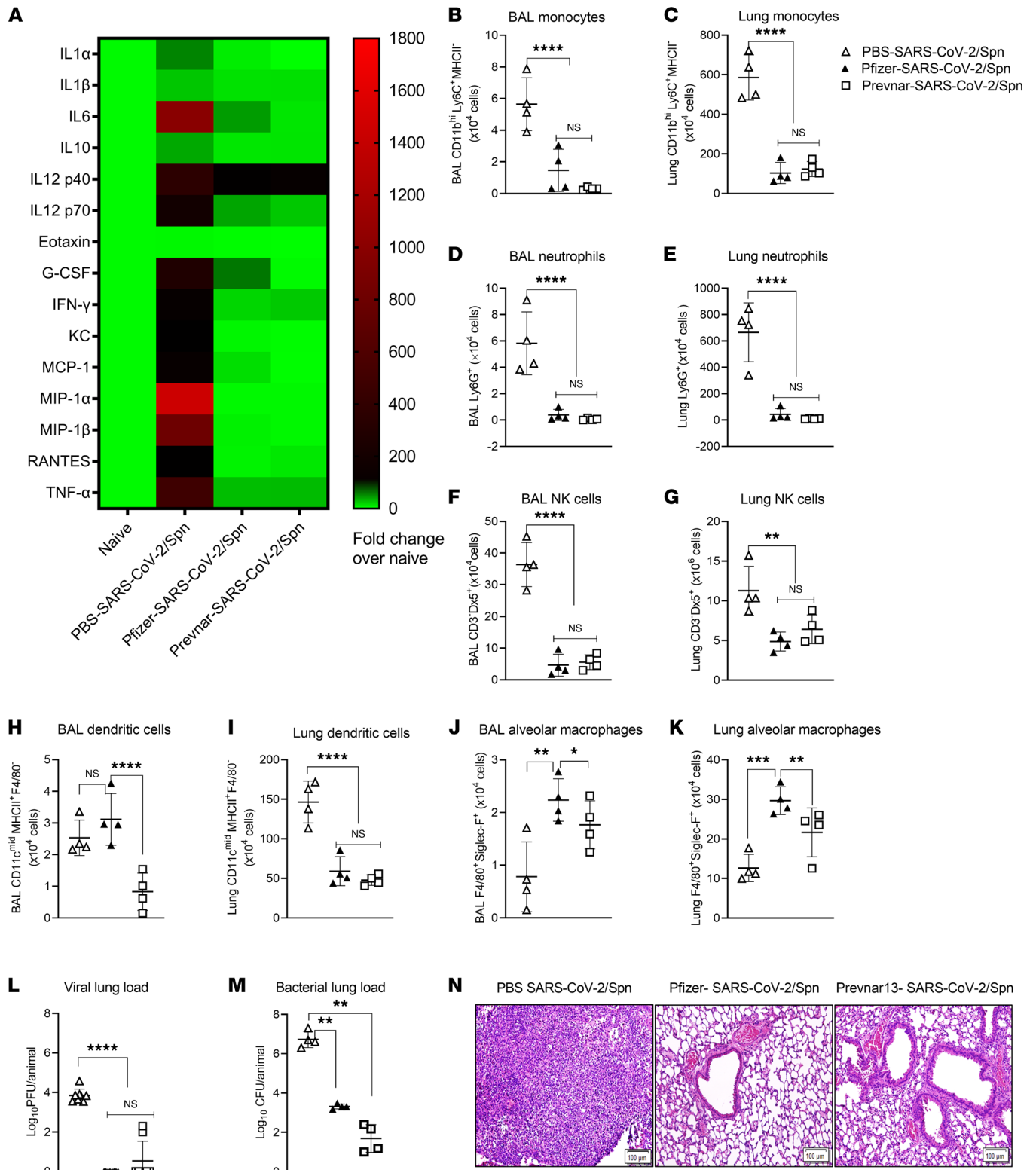


**Figure 6. Correlates of vaccine efficacy against SARS-CoV-2/*S. pneumoniae* coinfection in hACE2 mice.** (A) Cytokine levels in the BALF of SARS-CoV-2/*S. pneumoniae*-coinfected hACE2 mice. (B–K) Innate immune cell profiles in BAL and lung tissues from SARS-CoV-2/*S. pneumoniae*-coinfected hACE2 mice: (B and C) monocytes, (D and E) neutrophils, (F and G) NK cells, (H and I) dendritic cells, and (J and K) alveolar macrophages. *n* = 4 mice per group per experiment; each symbol represents a single mouse. (L) Viral PFU in lung homogenates. *n* = 4 mice per group. (M) Bacterial CFU in lung homogenates. *n* = 4 mice per group. (N) Representative H&E staining of lung tissues from PBS-SARS-CoV-2/*S. pneumoniae*, Pfizer-SARS-CoV-2/*S. pneumoniae*, and Pevnar13-SARS-CoV-2/*S. pneumoniae*-immunized coinfecting hACE2 mice. *n* = 3 mice per group. Original magnification,  $\times 20$ . Scale bar: 100  $\mu$ m. Data were analyzed by ANOVA with Tukey's multiple comparisons post hoc test. Data are representative of 2 independent experiments and are presented as mean  $\pm$  SD. \**P* < 0.05, \*\**P* < 0.01, \*\*\**P* < 0.001, \*\*\*\**P* < 0.0001. Spn, *S. pneumoniae*.

therapy are ongoing (23), and further studies in animals could determine whether protocols for GM-CSF treatment optimization could provide improved levels of protection.

We further investigated the efficacy of therapeutic and prophylactic mAb cytokine neutralization for prevention of lethal SARS-CoV-2/*S. pneumoniae* superinfection. We have previously shown that neutralization of respiratory IFN- $\alpha\beta$  and IFN- $\gamma$  signaling protects mice colonized with *S. pneumoniae* from subsequent influenza virus coinfection. The detrimental roles of IFN- $\alpha\beta$  and IFN- $\gamma$  have also been described in mice infected first with influenza virus followed by *S. pneumoniae* challenge (12, 43, 44). In addition, others have reported that lung cytokine neutralization could rescue hACE2 mice from lethal SARS-CoV-2 infection, particularly from tissue damage caused by the induction of IFN- $\gamma$  and TNF- $\alpha$  expression (24). However, in our infection models, including either SARS-CoV-2/*S. pneumoniae* coinfection or *S. pneumoniae*/SARS-CoV-2 coinfection, neutralization of IFN- $\gamma$  and TNF- $\alpha$ , neutralization of IFN- $\alpha\beta$  and TNF- $\alpha$ , or neutralization of all 3 cytokine pathways failed in each case to alter survival rates. We considered also testing the efficacy of IL-1 and IL-6 neutralization. Recent findings have supported the use of anti-IL-1/IL-1R and anti-IL-6 mAbs in patients with severe COVID-19 (45–47), and these treatments have been approved by the US Food and Drug Administration for emergency usage in hospitalized patients with COVID-19 with systemic inflammation. Testing the potential of neutralizing these cytokine pathways in combination with GM-CSF administration for prevention of lethality during SARS-CoV-2/*S. pneumoniae* coinfection would be of interest. Neutralization of proinflammatory cytokine pathways could be helpful in the prevention of lethal tissue damage observed during superinfection.

SARS-CoV-2 and *S. pneumoniae* vaccines are highly effective in both humans and mice for protection against COVID-19 and pneumococcal infection, respectively (26, 48). However, their possible efficacy against lethal coinfection is not known. Thus, we immunized mice with the Pfizer mRNA COVID-19 vaccine or the pneumococcal Prevnar13 vaccine, followed 3 weeks later with a homologous booster vaccine dose and then 1 week later with SARS-CoV-2/*S. pneumoniae* coinfection. This vaccination protocol induced robust antibody production against SARS-CoV-2 and pneumococcal polysaccharide but only provided approximately 50% protection against SARS-CoV-2/*S. pneumoniae* superinfection. Previous studies in humans (49) and mice (26) similarly demonstrated that vaccination with Prevnar alone provides approximately 50% protection against influenza virus/*S. pneumoniae* coinfection. However, dual vaccination against both SARS-CoV-2 and pneumococcus induced 100% survival in mice following coinfection. Vaccination correlated with decreased inflammatory cell and cytokine expression, reversal of alveolar macrophage depletion, decreased viral and bacterial loads, and reduced lung pathology.

Coinfection with influenza virus and SARS-CoV-2 might also result in synergistic lethality. It appears that coinfections with influenza virus are currently not a significant clinical problem, although measures to restrict COVID-19 have resulted in very low levels of seasonal influenza for the past 2 years. Considering this, in other studies, we also examined potential synergy between SARS-CoV-2 and influenza virus in the hACE2-transgenic mouse model. Like superinfection with SARS-CoV-2 and *S. pneumoniae*, we observed significant lethality after coinfection with sublethal challenge doses of SARS-CoV-2 and influenza virus given on days 0 and 6, regardless of the sequence of coinfection (unpublished observations). In future studies, it will be of interest to investigate the ability of GM-CSF or vaccination to protect against SARS-CoV-2/influenza virus coinfection.

In summary, we have shown that hACE2-transgenic mice coinfecting with SARS-CoV-2 and *S. pneumoniae* become highly susceptible to lethal pathogenesis compared with mice infected with low doses of either pathogen alone. Treatment with GM-CSF provided some benefit from pathology, while vaccination against both COVID-19 and *S. pneumoniae* resulted in 100% protection from SARS-CoV-2/*S. pneumoniae* coinfection. As pandemic-related restrictions are lifted and increases in common respiratory infections become more likely, SARS-CoV-2/*S. pneumoniae* superinfections may represent a significant new threat to human health. Our study further argues in favor of widespread COVID-19 and pneumococcal vaccination in the human population to prevent SARS-CoV-2-associated bacterial superinfections.

## Methods

**Mice.** Male and female hACE2 receptor–transgenic mice (K18-hACE2 mice) were purchased from The Jackson Laboratory, bred in the Albany Medical College Animal Resource Facility, and used at 6–8 weeks of age. Infected animals were housed in individually ventilated cages within the Albany Medical College ABSL-3 facility.

**Bacterial and viral strains.** SARS-CoV-2 virus (Coronavirus strain 2019-nCoV/USA-WA1/2020, no. NR-52281; BEI Resources, NIAID, NIH) was grown and titrated on Vero E6 cell monolayers using standard procedures (50). In brief, exponentially growing Vero E6 cells were washed with sterile PBS and infected with SARS-CoV-2 virus at an MOI of 0.01 for 1 hour at 37°C in 5% CO<sub>2</sub>. After 3 days, the virus particles were concentrated and purified using the Abcam PEG virus precipitation kit. A final virus stock was prepared in sterile PBS and stored at –80°C until use. Frozen stocks of *S. pneumoniae* A66.1 strain serotype 3 were used for bacterial infection.

**Coinfection of hACE2 mice.** Mice were anesthetized with a mixture of 20% ketamine (100 mg/mL), 5% xylazine (20 mg/mL), and 75% PBS and infected i.n. using an inoculation volume of 40 µL. For coinfection, the initial challenge was given on day 0, and secondary infection was given on day 6, except for *S. pneumoniae* colonization experiments, in which *S. pneumoniae* was inoculated i.n. into lightly anesthetized mice in a volume of 20 µL, and secondary SARS-CoV-2 infection was performed on day 2. Mice were infected with 10<sup>3</sup> PFU of SARS-CoV-2 and 10<sup>3</sup> CFU of *S. pneumoniae* in sterile PBS. Control groups of mice received equal volumes of PBS. Each mouse was weighed daily and observed for clinical signs.

BAL and lung tissues were collected from infected mice on day 7 and day 9 after infection. For the collection of BALF, mice were euthanized, a small incision was made on the trachea, and the lungs were lavaged 3 times with 1 mL cold sterile PBS using an 18-gauge BD tubing adapter. The BALF was spun at 500g for 5 minutes at 4°C and stored at –80°C until analysis.

**Cytokine analysis.** BAL samples were collected on days 7 and 9 from naive mice, mice infected with *S. pneumoniae* only or SARS-CoV-2 only, and coinfecting mice. Cytokines in BALF were analyzed by a 23-plex Luminex multiplex bead-based assay (Bio-Rad) following the manufacturer's recommendations.

**Flow cytometry analysis.** Cell populations were assessed in BAL and lungs. Lung tissues were cut into small pieces and digested with Liberase TL (1 mg/mL; Roche) and DNase I (10 mg/mL; MilliporeSigma) for 30 minutes at 37°C with gentle agitation. Single-cell suspensions were obtained by passage through a 70 µm mesh. This was followed by treatment with FcγRII/III block (2.4G2 mAb) for 15 minutes and staining with fluorescent mAbs and Fixable Viability Dye (eFluor 780; eBioscience) to differentiate live and dead cells. Antibodies used were anti-CD11b (clone M1/70, PERcpcy5.5, BD Biosciences), anti-CD11c (clone N418, Pac Blue, BioLegend), anti-Siglec-F (clone E50-2440, PE, BD Biosciences), anti-MHC class II (clone M5/114.15.2, Pac Orange, BioLegend), anti-F4/80 (Clone BM8, Pac Blue, Invitrogen), anti-Ly6C (clone HK 1.4, APC, eBioscience), anti-Ly6G (clone 1A8, FITC, BD Biosciences), anti-CD3 (clone 17A2, APC, BioLegend), anti-CD4 (clone GK 1.5, FITC, BioLegend), anti-CD8 (clone 53–6.7, PE, BD Biosciences), and anti-Dx5 (clone DX5, Pac Blue, BioLegend). Stained cells were fixed with 2% paraformaldehyde before removal from the BSL-3 facility and analysis was performed on a BD FACS Canto using FACSDiva software. The data were analyzed using FlowJo, version 10.

**Bacterial and viral loads.** Bacterial loads in lung homogenates of infected mice were determined as described previously (51). Briefly, lung homogenates were prepared in PBS and serial dilutions plated on blood agar plates, which were incubated at 37°C in 5% CO<sub>2</sub>. Bacterial colonies were enumerated 18–20 hours later. Quantification of replicating SARS-CoV-2 virion levels in lung samples was performed as described previously (50). Briefly, Vero E6 cell monolayers were washed with PBS and infected with cell-free lung homogenates for 1 hour at 37°C. The infected cell monolayers were then overlaid with DMEM supplemented with 2% FBS, penicillin/streptomycin, and 1% methylcellulose and incubated for 4 days to allow development of cytopathic effects. The cells were fixed with 10% formalin for 1 hour followed by staining with 1% crystal violet and counting of PFU under ×10 magnification.

**Histopathology.** Lung samples were collected and fixed in 10% formalin. 5 µm tissue sections were prepared and stained with H&E. Ten fields from each lung section were randomly chosen for analysis using an Olympus BX41 microscope (52). Images were obtained under ×20 magnification using CellSense software. Histology scoring was performed as described previously (52, 53).

**In vivo GM-CSF treatment.** Murine GM-CSF (Miltenyi Biotec) was administered i.n. at a dose of 10 µg/mouse in PBS to lightly anesthetized mice. Treatment was given 1 day before SARS-CoV-2 infection and then further treatments were continued on days 1, 3, 5, and 7.

**In vivo cytokine neutralization.** Murine IFN-αβ, IFN-γ, and TNF-α were neutralized by intraperitoneal inoculation of 500 µg/mouse MAR1-5A3 anti-IFN-αβR mAb (BioXCell), 600 µg/mouse XMG1.2 anti-IFN-γ mAb (BioXCell), and 500 µg/mouse TN3-19.12 anti-TNF-α mAb (Leinco Technologies Inc.) in 200 µL PBS. Control mice received equal amounts of irrelevant isotype-matched mAbs. The mAbs were

administered on days 1, 3, 5, 7, 9, and 11 after infection. All treatments were given in a double-blind manner, using antibody preparations coded by an independent investigator. Mortality and weight loss were recorded daily until day 20.

**Immunization.** Groups of mice were vaccinated intramuscularly with 3 µg Pfizer mRNA SARS-CoV-2 vaccine and/or 2.86 µg Pevnar13 *S. pneumoniae* polysaccharide conjugate vaccine (Pfizer). Unvaccinated control mice received PBS. Serum antibody titers were determined by ELISA using Maxisorp 96-well microplates (Thermo Fisher Scientific) coated with 100 ng/well SARS-CoV-2 recombinant spike protein S1+S2 (BioLegend, 793706) or 200 ng/well purified pneumococcal polysaccharide serotype 3 (US Type 3; ATCC) overnight at 4°C. The remaining ELISA procedures were performed as described previously (54). Antibody titers were determined by calculating the 50% maximal OD<sub>405nm</sub> values for each ELISA.

**Correlates of protection in vaccinated mice.** To assess the correlates of protection, mice were immunized against *S. pneumoniae* or SARS-CoV-2 and infected with SARS-CoV-2; then 6 days later, mice were challenged with *S. pneumoniae*. Three days following coinfection, cytokine levels, cell expression, bacterial/viral loads, and histopathology were assessed.

**Statistics.** All statistical analyses were performed using GraphPad Prism version 9.0. Comparisons of cytokine expression as well as cell population levels between multiple groups were analyzed by 2-way ANOVA with Tukey's multiple comparisons. *P* values of less than 0.05 were considered to be statistically significant.

**Study approval.** All animal studies were approved by the Albany Medical College Institutional Animal Use and Care Committee (protocol no. 20-04001) and were conducted according to the regulations for animal experiments at Albany Medical College.

## Author contributions

TKB and DWM conceived the ideas, designed the experiments, and wrote the manuscript. TKB, AKS, JLB, TNN, and SLS performed experiments and analysis. DWM acquired funding and provided supervision.

## Acknowledgments

Technical assistance for cytokine analyses and histopathology was provided by the Albany Medical College Immunology Core, within the Department of Immunology and Microbial Disease. This research was supported by the NIH grant R01 HL140496-01 (to DWM).

Address correspondence to: Dennis W. Metzger, Department of Immunology and Microbial Disease, Albany Medical College, 47 New Scotland Ave., MC-151, Albany, New York 12208, USA. Phone: 518.262.6750; Email: metzged@amc.edu.

1. Tsukamoto T, et al. Lung pathology of mutually exclusive co-infection with SARS-CoV-2 and Streptococcus pneumoniae. *Emerg Infect Dis.* 2021;27(3):919–923.
2. Lansbury L, et al. Co-infections in people with COVID-19: a systematic review and meta-analysis. *J Infect.* 2020;81(2):266–275.
3. Westblade LF, et al. Bacterial coinfections in coronavirus disease 2019. *Trends Microbiol.* 2021;29(10):930–941.
4. Russell CD, et al. Co-infections, secondary infections, and antimicrobial use in patients hospitalised with COVID-19 during the first pandemic wave from the ISARIC WHO CCP-UK study: a multicentre, prospective cohort study. *Lancet Microbe.* 2021;2(8):e354–e365.
5. Zhou F, et al. Clinical course and risk factors for mortality of adult inpatients with COVID-19 in Wuhan, China: a retrospective cohort study. *Lancet.* 2020;395(10229):1054–1062.
6. Lai CC, et al. Increased antimicrobial resistance during the COVID-19 pandemic. *Int J Antimicrob Agents.* 2021;57(4):106324.
7. Barman TK, et al. Sequential targeting of interferon pathways for increased host resistance to bacterial superinfection during influenza. *PLoS Pathog.* 2021;17(3):e1009405.
8. Umstead TM, et al. Lower respiratory tract delivery, airway clearance, and preclinical efficacy of inhaled GM-CSF in a postinfluenza pneumococcal pneumonia model. *Am J Physiol Lung Cell Mol Physiol.* 2020;318(4):L571–L579.
9. Baden LR, et al. Efficacy and safety of the mRNA-1273 SARS-CoV-2 vaccine. *N Engl J Med.* 2021;384(5):403–416.
10. Polack FP, et al. Safety and efficacy of the BNT162b2 mRNA COVID-19 vaccine. *N Engl J Med.* 2020;383(27):2603–2615.
11. Bao L, et al. The pathogenicity of SARS-CoV-2 in hACE2 transgenic mice. *Nature.* 2020;583(7818):830–833.
12. Sun K, Metzger DW. Inhibition of pulmonary antibacterial defense by interferon-gamma during recovery from influenza infection. *Nat Med.* 2008;14(5):558–564.
13. Sun K, Metzger DW. Influenza infection suppresses NADPH oxidase-dependent phagocytic bacterial clearance and enhances susceptibility to secondary methicillin-resistant Staphylococcus aureus infection. *J Immunol.* 2014;192(7):3301–3307.
14. Henry BM. COVID-19, ECMO, and lymphopenia: a word of caution. *Lancet Respir Med.* 2020;8(4):e24.
15. Ruan Q, et al. Clinical predictors of mortality due to COVID-19 based on an analysis of data of 150 patients from Wuhan, China. *Intensive Care Med.* 2020;46(5):846–848.

16. Davis BM, et al. Influenza and community-acquired pneumonia interactions: the impact of order and time of infection on population patterns. *Am J Epidemiol.* 2012;175(5):363–367.
17. Huang FF, et al. GM-CSF in the lung protects against lethal influenza infection. *Am J Respir Crit Care Med.* 2011;184(2):259–268.
18. Rosler B, Herold S. Lung epithelial GM-CSF improves host defense function and epithelial repair in influenza virus pneumonia—a new therapeutic strategy? *Mol Cell Pediatr.* 2016;3(1):29.
19. Sever-Chroneos Z, et al. GM-CSF modulates pulmonary resistance to influenza A infection. *Antiviral Res.* 2011;92(2):319–328.
20. Steinwede K, et al. Local delivery of GM-CSF protects mice from lethal pneumococcal pneumonia. *J Immunol.* 2011;187(10):5346–5356.
21. Subramaniam R, et al. Delivery of GM-CSF to protect against influenza pneumonia. *PLoS One.* 2015;10(4):e0124593.
22. Unkel B, et al. Alveolar epithelial cells orchestrate DC function in murine viral pneumonia. *J Clin Invest.* 2012;122(10):3652–3664.
23. Lang FM, et al. GM-CSF-based treatments in COVID-19: reconciling opposing therapeutic approaches. *Nat Rev Immunol.* 2020;20(8):507–514.
24. Karki R, et al. Synergism of TNF- $\alpha$  and IFN- $\gamma$  triggers inflammatory cell death, tissue damage, and mortality in SARS-CoV-2 infection and cytokine shock syndromes. *Cell.* 2021;184(1):149–168.
25. Huang Q, et al. A single-dose mRNA vaccine provides a long-term protection for hACE2 transgenic mice from SARS-CoV-2. *Nat Commun.* 2021;12(1):776.
26. Metzger DW, et al. Limited efficacy of antibacterial vaccination against secondary serotype 3 pneumococcal pneumonia following influenza infection. *J Infect Dis.* 2015;212(3):445–452.
27. Chen G, et al. Clinical and immunological features of severe and moderate coronavirus disease 2019. *J Clin Invest.* 2020;130(5):2620–2629.
28. Gao Y, et al. Diagnostic utility of clinical laboratory data determinations for patients with the severe COVID-19. *J Med Virol.* 2020;92(7):791–796.
29. Huang C, et al. Clinical features of patients infected with 2019 novel coronavirus in Wuhan, China. *Lancet.* 2020;395(10223):497–506.
30. Ragab D, et al. The COVID-19 cytokine storm; what we know so far. *Front Immunol.* 2020;11:1446.
31. Sun D, et al. Clinical features of severe pediatric patients with coronavirus disease 2019 in Wuhan: a single center's observational study. *World J Pediatr.* 2020;16(3):251–259.
32. Knoll R, et al. Monocytes and macrophages in COVID-19. *Front Immunol.* 2021;12:720109.
33. Zheng J, et al. Severe acute respiratory syndrome coronavirus 2-induced immune activation and death of monocyte-derived human macrophages and dendritic cells. *J Infect Dis.* 2021;223(5):785–795.
34. Amulic B, et al. Neutrophil function: from mechanisms to disease. *Annu Rev Immunol.* 2012;30:459–489.
35. Johansson C, Kirsebom FCM. Neutrophils in respiratory viral infections. *Mucosal Immunol.* 2021;14(4):815–827.
36. Bardeol BW, et al. The balancing act of neutrophils. *Cell Host Microbe.* 2014;15(5):526–536.
37. Bao C, et al. Natural killer cells associated with SARS-CoV-2 viral RNA shedding, antibody response and mortality in COVID-19 patients. *Exp Hematol Oncol.* 2021;10(1):5.
38. Borges RC, et al. Dendritic cells in COVID-19 immunopathogenesis: insights for a possible role in determining disease outcome. *Int Rev Immunol.* 2021;40(1–2):108–125.
39. Califano D, et al. Effects of influenza on alveolar macrophage viability are dependent on mouse genetic strain. *J Immunol.* 2018;201(1):134–144.
40. Ghoneim HE, et al. Depletion of alveolar macrophages during influenza infection facilitates bacterial superinfections. *J Immunol.* 2013;191(3):1250–1259.
41. Neupane AS, et al. Patrolling alveolar macrophages conceal bacteria from the immune system to maintain homeostasis. *Cell.* 2020;183(1):110–125.
42. Sun SH, et al. A mouse model of SARS-CoV-2 infection and pathogenesis. *Cell Host Microbe.* 2020;28(1):124–133.
43. Nakamura S, et al. Synergistic stimulation of type I interferons during influenza virus coinfection promotes Streptococcus pneumoniae colonization in mice. *J Clin Invest.* 2011;121(9):3657–3665.
44. Shahangian A, et al. Type I IFNs mediate development of postinfluenza bacterial pneumonia in mice. *J Clin Invest.* 2009;119(7):1910–1920.
45. Kyriazopoulou E, et al. Effect of anakinra on mortality in patients with COVID-19: a systematic review and patient-level meta-analysis. *Lancet Rheumatol.* 2021;3(10):e690–e697.
46. Yu SY, et al. Clinical efficacy and safety of interleukin-6 receptor antagonists (tocilizumab and sarilumab) in patients with COVID-19: a systematic review and meta-analysis. *Emerg Microbes Infect.* 2022;11(1):1154–1165.
47. CORIMUNO-19 Collaborative group. Effect of anakinra versus usual care in adults in hospital with COVID-19 and mild-to-moderate pneumonia (CORIMUNO-ANA-1): a randomised controlled trial. *Lancet Respir Med.* 2021;9(3):295–304.
48. Lopez Bernal J, et al. Effectiveness of Covid-19 vaccines against the B.1.617.2 (Delta) variant. *N Engl J Med.* 2021;385(7):585–594.
49. Madhi SA, et al. A role for Streptococcus pneumoniae in virus-associated pneumonia. *Nat Med.* 2004;10(8):811–813.
50. Singh AK, et al. Lack of active SARS-CoV-2 virus in a subset of PCR-positive COVID-19 congregate care patients. *J Clin Virol.* 2021;141:104879.
51. Barman TK, et al. In vitro and in vivo activities of a bi-aryl oxazolidinone, RBx 11760, against gram-positive bacteria. *Antimicrob Agents Chemother.* 2016;60(12):7134–7145.
52. Buchweitz JP, et al. Modulation of airway responses to influenza A/PR/8/34 by Delta9-tetrahydrocannabinol in C57BL/6 mice. *J Pharmacol Exp Ther.* 2007;323(2):675–683.
53. Caricchio R, et al. Effect of canakinumab vs placebo on survival without invasive mechanical ventilation in patients hospitalized with severe COVID-19: a randomized clinical trial. *JAMA.* 2021;326(3):230–239.
54. Lynch JM, et al. Increased protection against pneumococcal disease by mucosal administration of conjugate vaccine plus interleukin-12. *Infect Immun.* 2003;71(8):4780–4788.